Journal of King Saud University - Science 36 (2024) 103556

HOSTED BY

Contents lists available at ScienceDirect

Journal of King Saud University - Science

journal homepage: www.sciencedirect.com

Full Length Article

Therapeutic potential of Chemogenic Iron oxide Nanoparticles, its antioxidant and anti-Inflammatory effects with reduction of ankle joint swelling in BALB/c mice

Mubin Mustafa Kiyani [a,*], Sarah Sadiq [b], Maria Sarfraz [c], Chanda Javed [a], Maisra Azhar Butt [d], Hassan Burair Abbas [e], Hamza Rehman [d], Syed Ali Imran Bokhari [d]

[a] Shifa College of Medical Technology, Shifa Tameer-e-Millat University, Islamabad, Pakistan
[b] CMH Kharian Medical College, Kharian Cantt, Gujrat, National University of Medical Sciences, Rawalpindi, Pakistan
[c] Department of Biochemistry, Rawal Institute of Health Sciences, Shaheed Zulfiqar Ali Bhutto Medical University (SZABMU), Islamabad, Pakistan
[d] Department of Bioinformatics and Biotechnology, International Islamic University, Islamabad, Pakistan
[e] Department of Medicine, HITEC- Institute of Medical Sciences, National University of Medical Sciences, Rawalpindi, Pakistan

ARTICLE INFO

Keywords:
Antioxidants
Allopurinol
Iron oxide nanoparticles
Gout
Inflammation
Mice

ABSTRACT

Background: Gout is a form of inflammatory arthritis caused by excessive deposition of uric acid in the body and joints. Prolonged administration of uric acid lowering drugs have multiple side effects. Objectives: To investigate the antioxidant and anti-gout properties of iron oxide nanoparticles in hyperuricemic gouty mice. Methodology: Sol-Gel precipitation technique was used for chemogenesis of Iron oxide nanoparticles by using Ferrous Chloride (FeCl2) and Ferric chloride (FeCl3). Characterization was carried out by X-ray diffraction, SQUID magnetization, scanning electron microscopy(SEM) and energy-dispersive X-ray spectroscopy(EDX). Monosodium Urate crystals (MSUC) induced gout into the ankle joint of the mice. Iron oxide nanoparticles were orally administrated to the mice. To study the impact of Iron oxide nanoparticles biochemical analysis like total protein, antioxidant activity, and ankle diameter were conducted. Results: Results showed that oral administration of iron oxide nanoparticles had a beneficiary impact on gouty mice. The antioxidant activity were significantly improved by increasing levels of thiobarbituric acid reactive substance and reactive oxygen species in treated group with 250 mg/kg of body weight of iron oxide nanoparticles. Ankle diameter and levels of total protein were also reduced in treated groups. Conclusion: Current research indicates that Iron oxide nanoparticles have antioxidant as well as anti-gout effects in gouty mice. These results provide credence to the possibility of using Iron oxide nanoparticles as a gout alternative treatment. The potential therapeutic uses of iron oxide nanoparticles in human patients require more investigation.

1. Introduction

Nanoparticles are extraordinary small size particles with size ranges between 1 and 100 nm either in two or three dimensional orientation (Oborny, 2007). This unique nature of the nanoparticles are incredibly useful in drug delivery (Mudshinge, Deore, Patil, & Bhalgat, 2011). Having said of their nano size, they can easily approaches the targeted location within the human body and bypass the biological barriers. Nanoparticles can be engineered for transportation and to prevent the degradation of drugs and therapeutic substances and it also allow slow and control release of these loaded substances. Moreover the surface of nanoparticles can also be modified for target drug delivery particularly to tissues and cells. The improved and enhance target drug delivery lowers the risk of drugs side effects (A. Kumar & Thakur, 2022).

Iron Oxide nanoparticles consisting of large variety of polymorphs in nanomaterials with unique physiochemical characteristics. They may have 4 standardize principal polymorphic forms, hematite (α-Fe2O3), β-Fe2O3, maghemite (γ-Fe2O3) and ε-Fe2O3; similarly the iron (III) oxy-hydroxide also comprises four polymorphic forms which are recognize as goethite, akaganeite, lepidocrocite and feroxyhyte as α, β, γ and

* Corresponding author at: Shifa College of Medical Technology, Shifa Tameer-e-Millat University, Islamabad, Pakistan.
E-mail addresses: mubin.scmt@stmu.edu.pk (M. Mustafa Kiyani), Sarahsaddiq87@gmail.com (S. Sadiq), sarfarazmaria175@gmail.com (M. Sarfraz), chandajaved10033@gmail.com (C. Javed), maisrabutt70@gmail.com (M. Azhar Butt), hassan.burair@hitec-ims.edu.pk (H. Burair Abbas), hamzarehman51@gmail.com (H. Rehman), ali.imran@iiu.edu.pk (S. Ali Imran Bokhari).

https://doi.org/10.1016/j.jksus.2024.103556
Received 19 July 2024; Received in revised form 21 November 2024; Accepted 24 November 2024
Available online 6 December 2024

δ-FeOOH respectively. Interestingly, α-Fe2O3 is a well-known n-type semiconductor having bandgap Eg = 2.1 eV, prominent for an excellent chemical stability and reduce toxicity under normal existing conditions. Out of theses mentioned oxides, α-FeOOH and α-Fe2O3 have been popular for magnetic devices, catalysts, gas sensors, effective UV-blocking (Havenga et al., 2022) and photoelectrodes applications (Matinise et al., 2018). Moreover the green synthesized iron oxide nanoparticles has gain popularity due to its ecological friendly approach and improved the biocompatiability (Hassan et al., 2018; Khalil et al., 2017; Köçkar, Karaagac, Özel, & Materials, 2019), antimicrobial activity (Aisida et al., 2020; Madubuonu et al., 2020).

Gout, a painful joint inflammation, affects approximately 1% of the population, predominantly males (Wu et al., 2022). It occurs because monosodium urate crystals (MSUC) are gathered in the joints and surrounding tissues. Gout patients often exhibit hyperuricemia, characterized by raised uric acid levels in the blood (>70 lg/ml). Acute gout attacks can be triggered by factors like injury (Abhishek, Valdes, Jenkins, Zhang, & Doherty, 2017), exposure to cold, high food intake, and obesity (Tan, Farrar, Gaucher, Miner, & evolution, 2016). Uric acid is a necessary intermediate in the breakdown of purines, and its serum levels can rise due to various factors, including genetic factors and lifestyle choices. In most organisms, uric acid is transformed into allantoin, a soluble material, by the enzyme uricase. However, in primates, including humans, uricase activity is diminished due to gene mutation (Parthasarathy, Vivekanandan, & systems, 2018), resulting in the accumulation of uric acid in the body. Uric acid has the lowest solubility among purine byproducts, and its crystallization into MSUC is a critical factor in uric acid-mediated inflammation seen in gout. The inflammatory response stimulated by MSUC can lead to the development of tophi, which accumulates urate crystals in the tissues and joints (Kosugi, Nakagawa, Kamath, & Johnson, 2009). Some studies have evident that raised levels of soluble uric acid may be linked with conditions such as hypertension and certain cardiovascular diseases (S. Kumar et al., 2019).

The broad spectrum utilization of iron oxide nanoparticles within different applied scientific fields (O Karaagac, Hasirci, & Köçkar, 2024), such as controlled drug delivery systems, enzyme immobilization, and medical diagnostics, is more interesting area of research. Iron oxide nanoparticles demonstrate remarkable qualities in medicine with their exceptional characteristics like high surface area, magnetic susceptibility, and biocompatibility (Bhatia, Bhatia, & algae, 2016). The combine impact of nanotechnology and drug delivery system holds great prospective for improving the cure of enormous diseases, including those related to bone health and uric acid metabolism (Yang & Webster, 2009). Ongoing research and developmental efforts in this field have potential to uncover cutting-edge and unique therapeutics that can improve patient outcomes and quality of life (Oznur Karaagac, Kockar, Tanrisever, & magnetism, 2011; Oznur Karaagac, Kockar, & magnetism, 2012).

In this current study, researchers have synthesized iron nanoparticles to investigate their effects on the reduction of ankle diameter, antioxidant and anti-gout properties in a gouty mice model.

2. Material and methods

2.1. Synthesis of Iron oxide nanoparticles

The iron oxide nanoparticles was obtained using the Sol-Gel precipitation method. A 1:2 ratio of the two iron salts $FeCl_2$ and $FeCl_3$ were dissolved in continuous stirring 50 ml of deionized water and then 50 ml of 8.5 M NaOH solution were added drop by drop. When precipitates were formed then the resulting mixture were undergone the filtration process, the precipitates obtained were then washed multiple time with deionized water. After the complete washing the precipitate is then subjected to calcination at 100°C for overnight which was the main step for iron oxide nanoparticles formation. Powder form Iron oxide nanoparticles were obtained after overnight calcination which were grinded using a mortar and pestle. This whole process of Iron oxide nanoparticles synthesis is represented in Fig. 1 with slight modifications of previously conducted study by Karaagac and Kockar (Oznur Karaagac et al., 2012).

2.2. Characterization of nanoparticles

Multiple analytical methods were applied for characterization of synthesized iron oxide nanoparticles. These methods includes X-ray diffraction (XRD) analysis which was carried out by using AXS D8 device. Whereas the surface structural morphology was examined by using the scanning electron microscopy (SEM) made up of Hitachi S-4800 device. While the elemental analysis of the nanoparticles was analyzed by energy-dispersive X-ray spectroscopy (EDS) Carried on a Horiba 6853-H system. The magnetic properties of the prepared iron oxide nanoparticle sample were measured for nanoscale particles using a superconducting quantum interference device (SQUID) magnetometer, MPMS-XL from Quantum Design Inc USA. The measurements were taken across the magnetic field, negative 20,000 Oe to a positive 20,000 Oe at room temperature, 300k and 4k to obtain the values of saturation magnetization (M_s) and coercivity (H_c) (Oznur Karaagac, Köçkar, & Materials, 2022).

2.3. In Vivo studies

The animal model experiment was carried out after the authorization of the protocols from the institutional animal ethics review committee having File No. **XXXXXX** of **XXXXXX**.

2.4. Preparation of monosodium urate crystals (MSUC)

MSCU ware obtained by heating 1.68 g of uric acid with 0.001 M sodium hydroxide solution, with meticulous control of the pH range maintained at 7.0 to 7.2 using hydrochloric acid (HCl). After pH adjustment, the mixture was allowed to settle down undisturbed at room temperature for 24 h to MSUC formed then the supernatant was carefully removed, and crystals was rinsed with double distilled water multiple times. Microscopic analysis was carried out to verify the presence of needle-shaped MSUC in the sample (Getting, Christian, Flower, Perretti, & Rheumatism, 2002; Kiyani, Moghul, Butt, et al., 2022).

2.5. Preparation of allopurinol solution

The allopurinol suspension was created out by dissolution of a powdered tablet in deionized water and was administered to mice with hyperuricemia through oral gavage. The suspension dosage was tailored according to the average weight of mice within group 6.

2.6. Experimental design

The MSUC induced hyperuricemia experimental mice were divided into six groups, all receiving MSUC, except for the control group. MSUC were injected intra-articularly in left ankle and intra-peritoneal over three weeks and two weeks respectively at one-day intervals. Blood samples were evacuated regularly to monitor the mice's uric acid concentration. After the initial three-week period, the mice were subjected to oral administration of various concentrations of iron oxide nanoparticles, as specified in Fig. 2**.** Upon completion of the experiment, the animal model mice were euthanized; blood and tissue samples of Kidney, liver, and muscle were collected and preserved within paraffin blocks for subsequent analysis of tissue iron levels using atomic absorption spectroscopy and for histopathology determination (Kakkar, Das, & Viswanathan, 1984).

2.7. Measurement of ankle swelling

The digital Vernier caliper was used to quantify the swelling of ankle

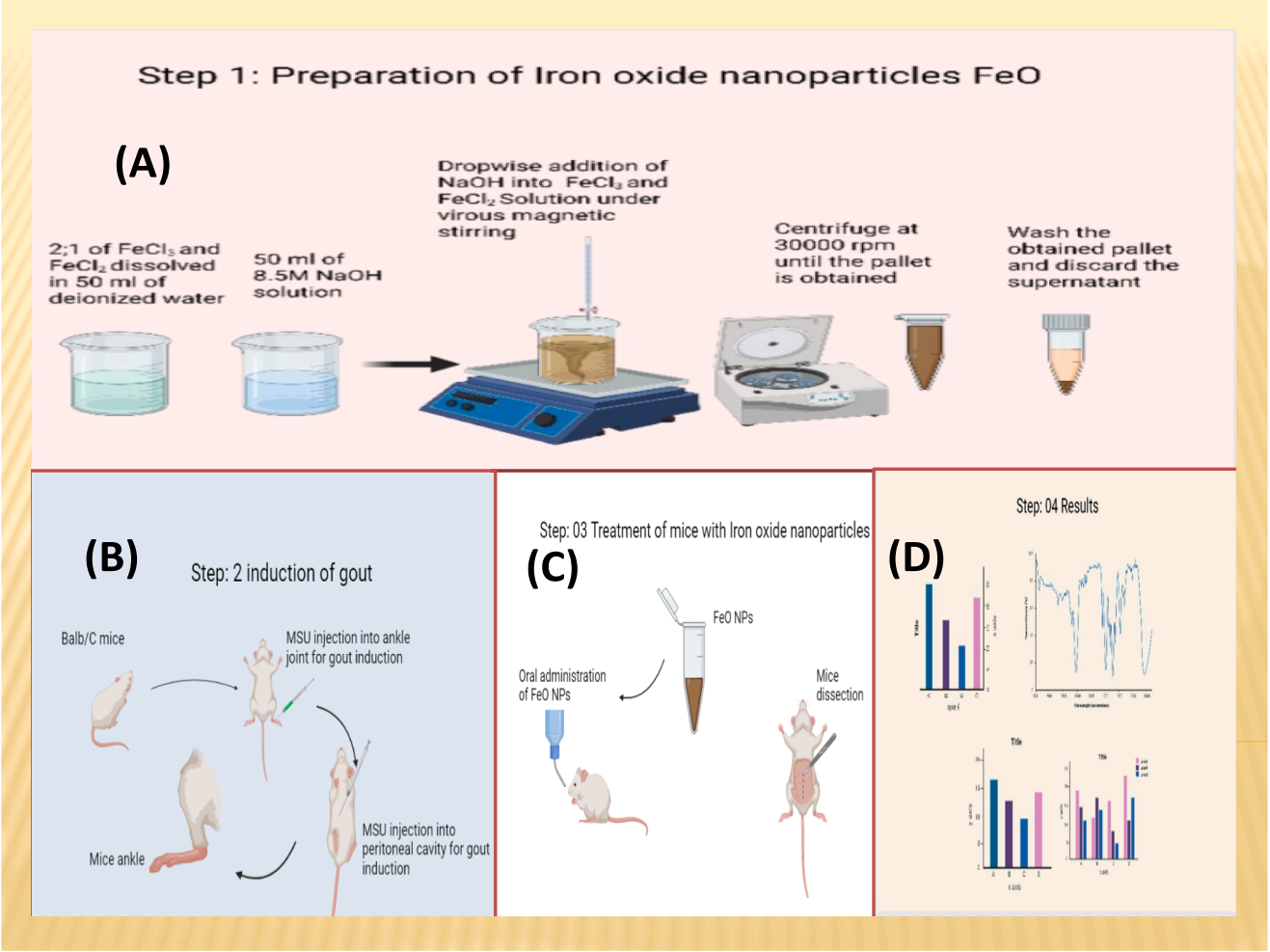

Fig. 1. Graphical abstract; (A) Synthesis and characterization of iron oxide nanoparticles, (B) Induction of gout, (C) Treatment of mice with iron oxide nanoparticles, (D) Results.

diameter in millimeter regularly pre and post treatment to analyze the effectiveness of given treatment. Weekly measurements of ankle diameter were shown in Table 1.

2.8. Total protein estimation

Total protein levels were estimated by purchasing commercially accessible kits from AMP Diagnostics AMEDA Labordiagnostik GmbH, Austria, as per manufacturer's instructions (Table 2).

2.9. Antioxidant activity

The antioxidant enzyme levels in the hepatic tissue of both control as well as treated animals were assessed.

2.9.1. SOD, POD, and CAT analysis

Superoxide dismutase (SOD) levels were determined following the protocol previously used by (Chance et al., 1957). The assay included 0.1 m1 1M phenazine methosulphate and 1.2 ml of sodium pyrophosphate buffer (pH 8.3, 0.052 Al). Using a Unicam SP 500 spectrophotometer, the chromogen in the butanol was analyzed at 560 nm using 0.3 ml 300 1M nitroblue tetrazolium and 0.2 ml NADH (180 1). Catalase (CAT) and peroxidase (POD) levels were investigated with slight modifications to the method outlined in (Vickers, 2017). The concentration of peroxidase and catalase was measured by spectrophotometry utilizing the molecular extinction.

2.9.2. ROS and TBARS

ROS levels were quantified using the protocol employed from the previous study (Vickers, 2017). Thiobarbituric reactive acid substances (TBARS) levels were analyzed by using a SmartSpec plus spectrophotometer described by Wright *et al* (Wright, Sutherland, & Metabolism, 2008).

2.10. Complete blood picture

The complete blood picture was estimated with the help of AMP diagnostic kits (AMEDA Labordiagonstik GmbH). It includes the white blood cells, red blood cells, platelets and hemoglobin count.

2.11. Statistical analysis

The statistical inquiry was performed by utilizing a one way analysis of variance (ANOVA), which was then followed by the Tukey Karamer test to compare all groups. The data were represented as mean ± standard error of the mean (SEM) and were calculated by using GraphPad Prism software (San Diego, CA, USA). Statistically $P < 0.05$ was considered significant level.

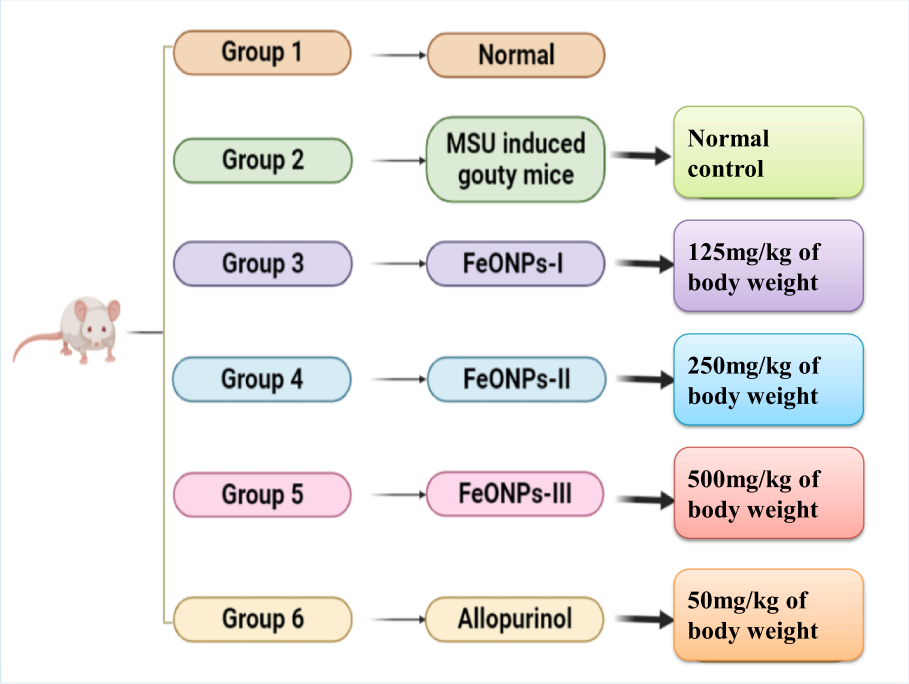

Fig. 2. Schematic diagram presenting dose administration in MSUC induced gouty mice.

Table 1
Week wise Measurement of Ankle Joint Diameter of Gouty Mice using Vernier Caliper (Before and After Treatment).

Groups (n = 6)	Measurements of the diameter (mm) of ankle joints			
	2nd Week	3rd Week	4th Week	5th week
Control group	2.49	2.54	2.65	2.56
MSUC group (−ve control)	5.85	6.84	6.87	6.95
Iron oxide nanoparticles (125 mg/kg of body weight)	5.29	5.97	3.34	2.94
Iron oxide nanoparticles (250 mg/kg of body weight)	5.13	6.23	3.25	2.66
Iron oxide nanoparticles (500 mg/kg of body weight)	5.76	6.21	3.20	2.53
Allopurinol (+ve control)	5.29	6.07	3.23	2.89

Table 2
Representation of the potential of iron oxide nanoparticles on Total protein in MSUC induced gouty mice.

Groups (n = 6)	Parameters
	Total protein (mg/dl)
Control group	5.09 ± 0.04
MSUC group (−ve control)	11.73 ± 0.47$^{a/b/c}$
Iron oxide nanoparticles (125 mg/kg of body weight)	6.61 ± 0.06$^{a/b/c}$
Iron oxide nanoparticles (250 mg/kg of body weight)	6.20 ± 0.04$^{a/b/c}$
Iron oxide nanoparticles (500 mg/kg of body weight)	3.74 ± 0.22$^{a/b/c}$
Allopurinol (+ve control)	2.51 ± 0.03$^{a/b/c}$

Expression of values are in Mean ± SD.
[a]Significantly different with comparison to the control group.
[b]Significantly different with comparison to the MSUC group.
[c]Significantly different with comparing to the allopurinol group.

3. Results

3.1. Characterization of nanoparticles

The X-ray diffraction analysis of the produced iron oxide nanoparticles corresponds to hematite indicates several Bragg reflections at different Bragg angles, as demonstrated in Fig. 3. Hematite exhibits a rhombohedral crystal structure with Fe^{3+} ions occupying octahedral coordination sites in a hexagonal close-packed array of oxygen ions. According to the previous study (Kiyani, Moghul, Butt, et al., 2022) the intense peak observed at around 2θ of 35.6748 corresponds to the (104) plane, characteristic of hematite α-Fe_2O_3 as per JCPDS card no. 33–0664. Moreover additional peaks further support its identification and is aligned with the electronic valence of Fe^{3+}, which confirms trivalent oxidation state of iron within the hematite phase. The estimated particle size was to be 58.64 nm by using the Debye-Scherrer equation. The SEM images showed morphological spherical shape with minimal agglomeration of synthesized iron oxide nanoparticles with approximately 64 nm in size as depicted in Fig. 4 **(a)** Moreover, energy-dispersive X-ray (EDS) established the occurrence of iron in the desired quantity, along with traces of other elements like chloride and sodium, EDS showcases in Fig. 4 **(b).** The magnetic hysteresis curve for the iron oxide nanoparticle sample is given in Fig. 5. The results presented in the measurements show weak dependence on magnetic fields and negligible hysteresis at low magnetic fields. The saturation magnetization M_s was resolved to be approximately 0.700 emu g^{-1}. H_c covering the magnetic field necessary to reduce the magnetization to zero after saturation was calculated to be −40.08 Oe. These results indicate the assumption made here that the nanoparticles are superparamagnetic as indicated by the fact that they have very low coercivity and zero remanent magnetization.

3.2. Biochemical analysis

After the dissection of the animals, blood and tissue samples were evacuated for further biochemical analysis. These biochemical analysis includes antioxidant analysis and total protein estimation.

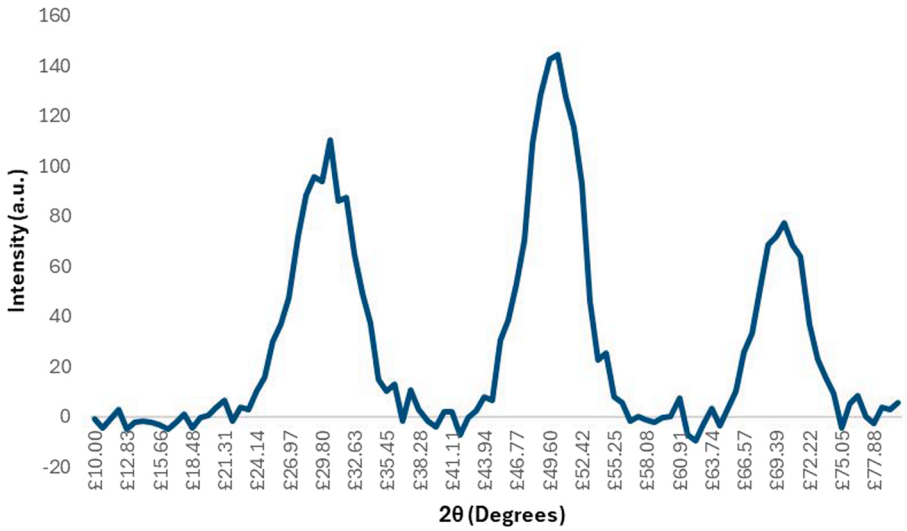

Fig. 3. X-ray diffraction pattern (XRD) of synthesized Iron oxide nanoparticles.

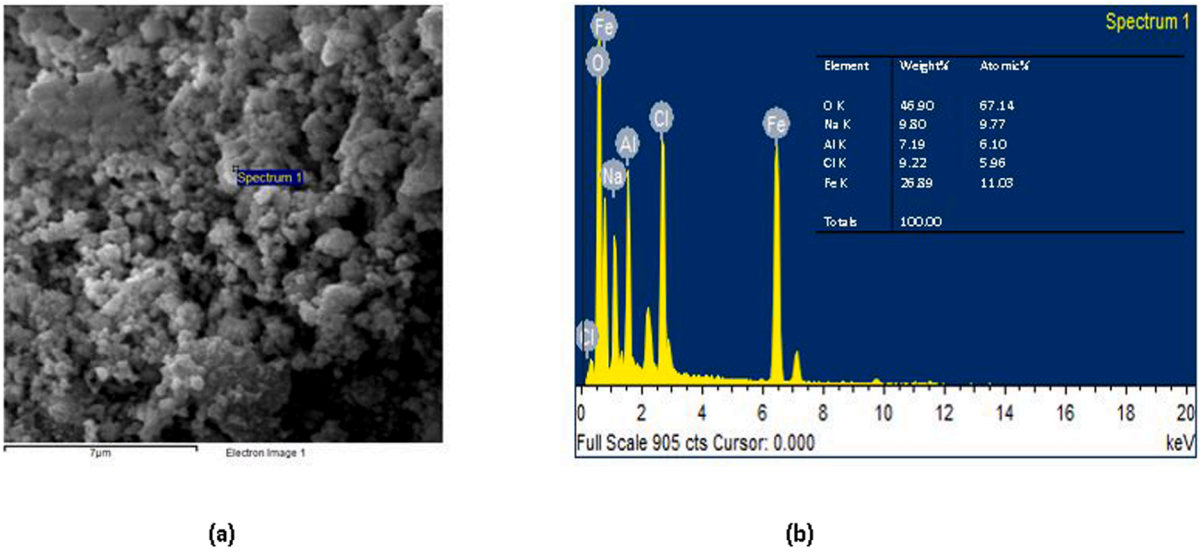

(a) (b)

Fig. 4. **(a)** Scanning Electron Microscope (SEM) image of synthesized Iron oxide nanoparticles **(b)** Energy dispersive X-ray spectroscopy pattern of synthesized Iron oxide nanoparticles.

3.2.1. Total protein estimation

A significant raise levels of the total protein content was observed when compared with the control group. However, all groups which were treated with Iron oxide nanoparticles represents a significant drop levels of total proteins in comparison to the control, MSUC and allopurinol treated group Table 2.

3.2.2. SOD, POD, and CAT

While comparing with the control, the levels of SOD were significantly higher in MSUC group. Whereas, SOD levels in all treated groups were decreased significantly as compared to the MSUC group. Similarly, the groups which were treated with 125mg/kg and 250mg/kg showed significant low in SOD levels in comparison with the allopurinol treated group.

Similarly, the levels of POD decreased significantly in the MSUC group as compared to the control. While the group undergone treatment with 500mg of Iron oxide nanoparticles showed no significant change in POD levels as compared to the control, MSUC, and allopurinol treated groups, whereas Iron oxide nanoparticles treated groups have significant increase in POD levels as compared to the MSUC group. The 125mg/kg of Iron oxide nanoparticles treated group exhibited significant changes in POD levels in comparison to the allopurinol treated group.

The level of CAT were decreased significantly in MSUC group compared with the control group. Whereas, 125mg/kg of Iron oxide nanoparticles treated group showed significant increase in CAT levels with the comparison of MSUC and allopurinol treated groups. All other treated groups showed significant increase in CAT levels with comparison to the MSUC group. Table 3 represents the values of SOD, POD, and CAT.

3.2.3. ROS and TBARS

The assessment of reactive oxygen species in MSUC group revealed a substantial raised in values with comparison to the control group. The Iron oxide nanoparticles treated groups exhibited a significant reduction in ROS levels with comparison to the control, MSUC, and allopurinol treated groups. Moreover, the TBARS evaluations of the MSUC group demonstrated a notable raised in values in comparison to control, while

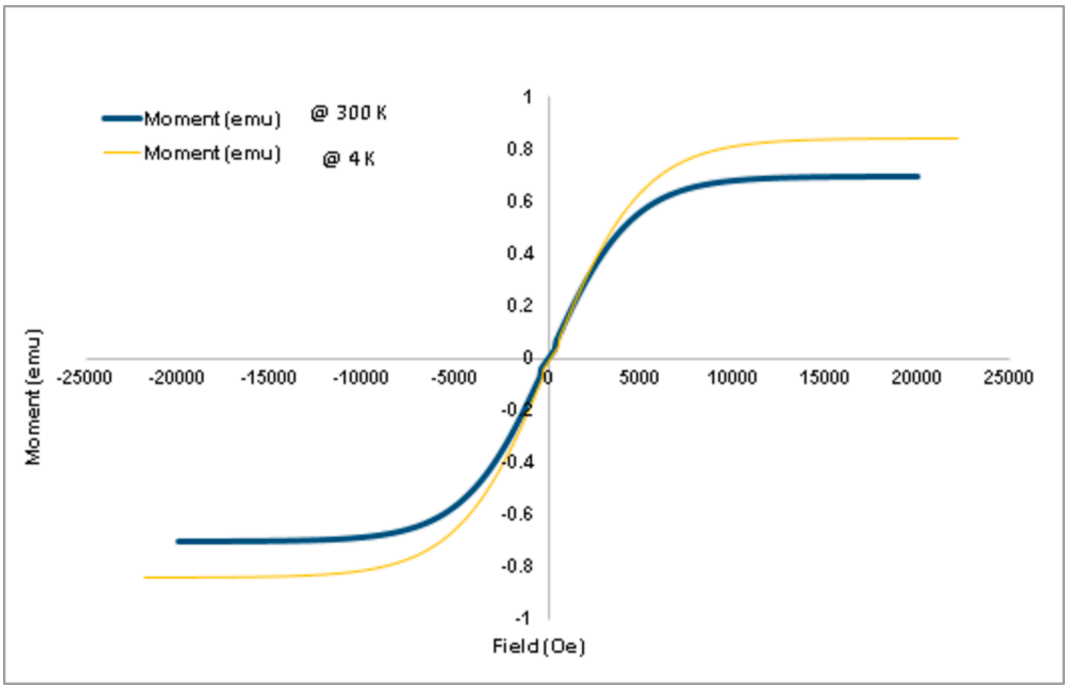

Fig. 5. Hysterisis Plot for SQUID analysis showing M vs. H for iron oxide nanoparticle at 300 and 4 K.

Table 3
Illustration of the potential of iron oxide nanoparticles on SOD, POD, CAT, ROS and TBARS in MSUC induced gouty mice.

Groups (n = 6)	Parameters				
	SOD (U/min)	POD (U/min)	CAT (U/min)	ROS (U/min)	TBARS (mmol/min/mg)
Control group	35.80 ± 0.43	3.05 ± 0.3	3.06 ± 0.17	1.58 ± 0.04	4.20 ± 0.07
MSUC group (−ve control)	21.51 ± 4.05[a]	1.10 ± 0.8[a]	1.56 ± 0.18[a]	3.56 ± 0.31[a]	15.38 ± 0.16[a]
Iron oxide nanoparticles (125 mg/kg of body weight)	27.01 ± 0.8[a/b/c]	1.36 ± 0.05[c]	2.33 ± 0.19[a/b/c]	1.78 ± 0.62[a/b/c]	2.25 ± 0.01[a/b/c]
Iron oxide nanoparticles (250 mg/kg of body weight)	28.46 ± 0.9[a/b/c]	3.15 ± 0.5[a/b]	3.17 ± 0.06[b]	1.37 ± 0.08[a/b/c]	2.44 ± 0.02[a/b/c]
Iron oxide nanoparticles (500 mg/kg of body weight)	34.94 ± 0.3[b]	3.33 ± 0.2[b]	3.37 ± 0.09[b]	1.67 ± 0.15[a/b/c]	4.45 ± 0.03[a/b/c]
Allopurinol (+ve control)	34.87 ± 0.5	2.80 ± 0.76[b]	3.27 ± 0.61[b]	2.51 ± 0.27[a/b/c]	3.64 ± 0.06[a/b/c]

Expression of values are in Mean ± SD.
[a] Significantly different with comparison to the control group.
[b] Significantly different with comparison to the MSUC group.
[c] Significantly different with comparing to the allopurinol group.

Iron oxide nanoparticles treated group exhibited a significant lowering in TBARS levels as compared to the control, MSUC, and allopurinol treated groups. The specific details can be observed in Table 3.

3.2.4. *Complete blood picture*

The WBCs count of the MSUC group was significantly raised ($P < 0.05$) with comparison to other treatment groups. On the other hand the RBCs count of Allopurinol group presented a significant difference ($P < 0.001$) with comparison to other groups. The detail of blood parameters is given in Table 4.

4. Discussion

The findings of the current study demonstrated that Iron oxide nanoparticles show promise in the treatment of gout in mice resulting from hyperuricemia, even at lower concentrations, while minimizing excessive damage to cells. Additionally, various biochemical tests were performed in this research work to assess the impact of Iron oxide nanoparticles on mice. Dextran or starch is commonly employed as a stabilizing agent in forming iron oxide nanoparticles to create a system that can disperse in water (LaConte, Nitin, & Bao, 2005). In an earlier study, the impact of injected Iron oxide nanoparticles on oxidative stress in various tissues and monitoring changes in hepatic enzymes as a measuring parameter of liver function was assessed. During investigations, a gradual rise in serum iron levels over one week was followed by a slow drop down, indicating that the elimination of magnetic NPs from the body takes longer than three weeks. The increase in serum iron levels can be attributed to several concurrent processes, including the breakdown of injected iron particles, subsequent binding of iron to various type of serum proteins like transferrin and re-dispersion of bound iron to body cells and tissues, and eventual elimination. The study suggests that most body iron exists in the bound state due to its slow clearing kinetics (Jain, Reddy, Morales, Leslie-Pelecky, & Labhasetwar, 2008).

One of the previous research observed that administration of silver oxide nanoparticles resulted in a notable elevation in protein estimation and lipid profile values in a group of gouty mice induced by MSUC. The raised protein levels indicated the magnitude of the response of inflammation, which is closely linked to oxidative stress (Kiyani, Moghul, Javed, et al., 2022). A separate study concluded that administration of ZnO-NPs to hyperuricemia mice model with gouty arthritis resulted in a considerable reduction in levels of blood uric acid. Moreover, the lipid profile tests demonstrated that the treatment with nanoparticles effectively lowered cholesterol and LDL levels with comparison to the control group. However, both the nanoparticles-treated and allopurinol-treated groups exhibited increased in hepatic enzymes

Table 4
Representation of the potential of iron oxide nanoparticles on Complete Blood Picture in MSUC induced gouty mice.

Group (n = 6)	WBCs 10^3/ mm^3	RBCs ml/mm^3	Hb g/dl	Hematocrit %	MCV F1	Platelets $10^3/mm^3$	RDW CV %
Normal Range	4–10	4.50–6.00	11–15	40–50	76–92	150–450	11.5–16
Control	7.21 ± 1.1^{c}	7.28 ± 0.2^{b}	12.1 ± 0.98^{bc}	190.50 ± 2.6^{d}	85.50 ± 2.46^{d}	300.8 ± 94.6^{f}	20.83 ± 2.33^{c}
MSUC group (−ve control)	37.63 ± 4.4^{g}	8.13 ± 1.3^{c}	9.83 ± 1.93^{a}	186.33 ± 3.1^{d}	49.83 ± 4.66^{a}	187.6 ± 46.9^{g}	20.83 ± 2.43^{c}
Iron oxide nanoparticles (125 mg/kg of body weight)	8.5 ± 0.41^{d}	7.22 ± 0.9^{b}	11.82 ± 2.12^{b}	175.50 ± 2.0^{cd}	59.00 ± 4.92^{b}	855 ± 30.3^{c}	24 ± 3.11^{d}
Iron oxide nanoparticles (250 mg/kg of body weight)	16.6 ± 2.0^{f}	7.40 ± 1.4^{bc}	14.13 ± 2.41^{d}	106.50 ± 3.8^{b}	63.50 ± 1.82^{bc}	907.3 ± 25.5^{a}	15.16 ± 1.21^{a}
Iron oxide nanoparticles (500 mg/kg of body weight)	5.23 ± 0.53^{b}	6.29 ± 0.9^{a}	13.17 ± 1.83^{c}	89.50 ± 2.1^{a}	73.17 ± 2.11^{c}	350.8 ± 101.5^{e}	15 ± 1.44^{a}
Allopurinol (+ve control)	7.48 ± 0.20^{e}	7.73 ± 0.8^{bc}	11.43 ± 1.09^{b}	147.00 ± 4.2^{c}	60.00 ± 4.2^{ab}	890 ± 141.4^{b}	24 ± 3.23^{d}

Expression of values are in Mean ± SD.
[a] Significantly different with comparison to the control group.
[b] Significantly different with comparison to the MSUC group.
[c] Significantly different with comparing to the allopurinol group.

concentrations.

Nonetheless, histopathological examination of kidney, liver and muscle tissues revealed no noticeable variations. This research provides evidence supporting the potential of orally given iron oxide nanoparticles in reducing the concentration of uric acid, cholesterol as well as LDL of the blood (Kiyani et al., 2019). In a previous conducted research, it was reported that CuO nanoparticle administration at different concentrations reduced serum ankle swelling in gouty mice with comparison to the negative control group (Kiyani et al., 2020), and these results are similar to our findings that Iron oxide nanoparticles administration reduced swelling in all treated groups.

5. Conclusion

This research results represents that low concentrations of Iron oxide nanoparticles hold potential as a prospective remedy for gouty arthritis in mice. Administering gout-afflicted mice with Iron oxide nanoparticles at 125, 250 and 500 mg/kg of body weight showcased antioxidative effects, signifying their possible therapeutic application in gout treatment. Moreover, Iron oxide nanoparticles demonstrated the capacity to lower total protein levels, suggesting reduced inflammation associated with gout.

CRediT authorship contribution statement

Mubin Mustafa Kiyani: Writing – original draft, Methodology, Conceptualization. **Sarah Sadiq:** Formal analysis, Data curation, Conceptualization. **Maria Sarfraz:** Investigation, Funding acquisition, Formal analysis. **Chanda Javed:** Resources, Methodology, Investigation. **Maisra Azhar Butt:** Software, Resources, Project administration. **Hassan Burair Abbas:** Project administration, Investigation, Funding acquisition. **Hamza Rehman:** Validation, Software, Project administration. **Syed Ali Imran Bokhari:** Writing – review & editing, Visualization, Validation, Supervision.

Funding

This research was conducted without any external funding.

Declaration of competing interest

The authors declare that they have no known competing financial interests or personal relationships that could have appeared to influence the work reported in this paper.

Acknowledgments

This manuscript constitutes a segment of Mubin Mustafa's doctoral dissertation. The authors thank the International Islamic University Islamabad, Pakistan and the National Institute of Health, Islamabad, Pakistan, for providing animal housing facilities.

Ethics Approval

Ethical approval letter has been taken from IRB of International Islamic University Islamabad Pakistan under File No. IBBC-IIUI-03.

Consent for Publication

All authors are mutually agreed for publication.

Appendix A. Supplementary material

Supplementary data to this article can be found online at https://doi.org/10.1016/j.jksus.2024.103556.

Data availability

Data will be made available on request.

The data that support the findings of this study are available from the corresponding author upon reasonable request.

References

Abhishek, A., Valdes, A.M., Jenkins, W., Zhang, W., Doherty, M., 2017. Triggers of acute attacks of gout, does age of gout onset matter? A primary care based cross-sectional study. PLoS One 12 (10), e0186096.

Aisida, S.O., Madubuonu, N., Alnasir, M.H., Ahmad, I., Botha, S., Maaza, M., Ezema, F.I., 2020. Biogenic synthesis of iron oxide nanorods using Moringa oleifera leaf extract for antibacterial applications. Appl. Nanosci. 10, 305–315.

Bhatia, S., & Bhatia, S. (2016). Nanoparticles types, classification, characterization, fabrication methods and drug delivery applications. Natural polymer drug delivery systems: Nanoparticles, plants, and algae, 33–93.

Chance, B., Maehly, A., Colowick, S., Kaplan, N. J. S. C., Kaplan, N., & Academic Press, I. N. Y., NY, USA. (1957). Methods in enzymol. 4, 273.

Getting, S.J., Christian, H.C., Flower, R.J., Perretti, M., 2002. Activation of melanocortin type 3 receptor as a molecular mechanism for adrenocorticotropic hormone efficacy in gouty arthritis. Arthritis Rheum. 46 (10), 2765–2775.

Hassan, D., Khalil, A.T., Saleem, J., Diallo, A., Khamlich, S., Shinwari, Z.K., Maaza, M., 2018. Biosynthesis of pure hematite phase magnetic iron oxide nanoparticles using floral extracts of Callistemon viminalis (bottlebrush): their physical properties and novel biological applications. Artif. Cells Nanomed. Biotechnol. 46 (sup1), 693–707.

Havenga, D., Akoba, R., Menzi, L., Azizi, S., Sackey, J., Swanepoel, N., Maaza, M., 2022. From Himba indigenous knowledge to engineered Fe2O3 UV-blocking green nanocosmetics. Sci. Rep. 12 (1), 2259.

Jain, T.K., Reddy, M.K., Morales, M.A., Leslie-Pelecky, D.L., Labhasetwar, V., 2008. Biodistribution, clearance, and biocompatibility of iron oxide magnetic nanoparticles in rats. Mol. Pharm. 5 (2), 316–327.
Kakkar, P., Das, B., & Viswanathan, P. N. (1984). A modified spectrophotometric assay of superoxide dismutase.
Karaagac, O., Kockar, H., Tanrisever, T., 2011. Properties of iron oxide nanoparticles synthesized at different temperatures. J. Supercond. Nov. Magn. 24, 675–678.
Karaagac, O., Hasirci, C., Köçkar, H., 2024. Optimum saturation magnetization of superparamagnetic iron oxide nanoparticles for versatile applications. Acta Phys. Pol. A 146 (2), 154–164.
Karaagac, O., Kockar, H., 2012. Effect of synthesis parameters on the properties of superparamagnetic iron oxide nanoparticles. J. Supercond. Nov. Magn. 25, 2777–2781.
Karaagac, O., Köçkar, H., 2022. Improvement of the saturation magnetization of PEG coated superparamagnetic iron oxide nanoparticles. J. Magn. Magn. Mater. 551, 169140.
Khalil, A.T., Ovais, M., Ullah, I., Ali, M., Shinwari, Z.K., Maaza, M., 2017. Biosynthesis of iron oxide (Fe2O3) nanoparticles via aqueous extracts of Sageretia thea (Osbeck.) and their pharmacognostic properties. Green Chem. Lett. Rev. 10 (4), 186–201.
Kiyani, M.M., Butt, M.A., Rehman, H., Ali, H., Hussain, S.A., Obaid, S., Bokhari, S.A.I., 2019. Antioxidant and anti-gout effects of orally administered zinc oxide nanoparticles in gouty mice. J. Trace Elem. Med Biol. 56, 169–177.
Kiyani, M.M., Rehman, H., Hussain, M.A., Jahan, S., Afzal, M., Nawaz, I., Bokhari, S.A.I., 2020. Inhibition of hyperuricemia and gouty arthritis in BALB/c mice using copper oxide nanoparticles. Biol. Trace Elem. Res. 193, 494–501.
Köçkar, H., Karaagac, O., Özel, F., 2019. Effects of biocompatible surfactants on structural and corresponding magnetic properties of iron oxide nanoparticles coated by hydrothermal process. J. Magn. Magn. Mater. 474, 332–336.
Kosugi, T., Nakagawa, T., Kamath, D., Johnson, R.J., 2009. Uric acid and hypertension: an age-related relationship? J. Hum. Hypertens. 23 (2), 75–76.
Kumar, A., & Thakur, A. (2022). Use of Nanoparticles to Combat COVID-19. In *Handbook of Research on Green Synthesis and Applications of Nanomaterials* (pp. 412-440). IGI Global.
Kumar, S., Singh, R., Zhu, G., Yang, Q., Zhang, X., Cheng, S., Liu, F.Z., 2019. Development of uric acid biosensor using gold nanoparticles and graphene oxide functionalized micro-ball fiber sensor probe. IEEE Trans. NanoBiosci. 19 (2), 173–182.
LaConte, L., Nitin, N., Bao, G., 2005. Magnetic nanoparticle probes. Mater. Today 8 (5), 32–38.
Madubuonu, N., Aisida, S.O., Ahmad, I., Botha, S., Zhao, T.K., Maaza, M., Ezema, F.I., 2020. Bio-inspired iron oxide nanoparticles using Psidium guajava aqueous extract for antibacterial activity. Appl. Phys. A 126, 1–8.
Matinise, N., Kaviyarasu, K., Mongwaketsi, N., Khamlich, S., Kotsedi, L., Mayedwa, N., Maaza, M., 2018. Green synthesis of novel zinc iron oxide (ZnFe2O4) nanocomposite via Moringa Oleifera natural extract for electrochemical applications. Appl. Surf. Sci. 446, 66–73.
Mudshinge, S.R., Deore, A.B., Patil, S., Bhalgat, C.M., 2011. Nanoparticles: Emerging carriers for drug delivery. Saudi Pharm. J. 19 (3), 129–141.
Oborny, M. C. (2007). *Nanotechnology: Industrial Hygiene Challenges and Recommended Practices* (No. SAND2007-7100C). Sandia National Lab.(SNL-NM), Albuquerque, NM (United States).
Parthasarathy, P., Vivekanandan, S., 2018. Urate crystal deposition, prevention and various diagnosis techniques of GOUT arthritis disease: a comprehensive review. Health Inf. Sci. Syst. 6, 1–13.
Tan, P.K., Farrar, J.E., Gaucher, E.A., Miner, J.N., 2016. Coevolution of URAT1 and uricase during primate evolution: implications for serum urate homeostasis and gout. Mol. Biol. Evol. 33 (9), 2193–2200.
Vickers, N.J., 2017. Animal communication: when i'm calling you, will you answer too? Curr. Biol. 27 (14), R713–R715.
Wright, D., Sutherland, L., 2008. Antioxidant supplemention in the treatment of skeletal muscle insulin resistance: potential mechanisms and clinical relevance. Appl. Physiol. Nutr. Metab. 33 (1), 21–31.
Wu, Z.D., Yang, X.K., He, Y.S., Ni, J., Wang, J., Yin, K.J., Pan, H.F., 2022. Environmental factors and risk of gout. Environ. Res. 212, 113377.
Yang, L., Webster, T.J., 2009. Nanotechnology controlled drug delivery for treating bone diseases. Expert Opin. Drug Deliv. 6 (8), 851–864.

Further reading

Kiyani, M.M., Moghul, N.B., Butt, M.A., Rehman, H., Masood, R., Rajput, T.A., Bokhari, S.A.I., 2022a. Anti-hyperuricemic effect of iron oxide nanoparticles against monosodium urate crystals induced gouty arthritis in BALB/c mice. Biol. Trace Elem. Res. 200 (4), 1659–1666.
Kiyani, M.M., Moghul, N.B., Javed, A., Butt, M.A., Abbas, H.B., Rehman, H., Bokhari, S. A.I., 2022b. In vivo effects of orally administered different concentrations of silver oxide nanoparticles in hyperuricemic mice. Biol. Trace Elem. Res. 1–11.